

**Fig. 2** The sunlight control of magnetic hysteresis loops study in PV/PMA heterostructures on flat conditions. (a) The  $H_c$  dependence of the thickness of the Co layer with (red) and without (blue) sunlight illumination. (b) The angular dependence of  $H_c$  without sunlight illumination (dark, red), under 1 sun (blue), 2 suns illumination (green), and back to dark conditions (re-dark, black). (c) The VSM measured magnetic hysteresis loops with (red) and without (blue) sunlight illuminations on flat conditions. (d) The magnetization switching with sunlight illumination turn on and off with magnetic bias assistance.

purchased from 1-Material Chemscitech Inc. (Canada). Lastly, a 3 nm Pt layer was deposited as the top electrode.

## 2.2 *In situ* magnetic property measurement

The *in situ* VSM measurement was taken with a LakeShore 7404 VSM system. The device was attached to a rotator, which shows the angle between the film plane and the applied magnetic field. The frequency of the TE 011 mode microwave was 9200 MHz. Devices were illuminated under AM 1.5 G ( $100 \text{ mW}\cdot\text{cm}^{-2}$ ) using a PL-XQ500W Xenon lamp solar simulator. The intensity of sunlight illumination is  $200 \text{ mW}\cdot\text{cm}^{-2}$  (2 suns).

## 3 Results and discussion

Figure 1(c) shows the magnetic hysteresis ( $M-H$ ) loops measured by vibrating sample measurements (VSM) of OPV/Pt (0.8 nm)/Co (0.7 nm)/Pt (2.75 nm) PMA heterostructure on the PET substrate at the flat conditions. Both in-plane (IP) and out-of-plane (OP)  $M-H$  loops are measured to identify a typical PMA, and the OP  $M-H$  loop is along the magnetic easy-axis compared

to the IP  $M-H$  loop. The Co thickness is carefully optimized to establish appropriate PMA strength for sunlight tuning, where too strong PMA is challenging to be manipulated.

Under sunlight illumination up to  $200 \text{ mW}\cdot\text{cm}^{-2}$ , referring to two standard suns, the  $H_c$  of the PMA  $M-H$  loops is significantly reduced, as demonstrated in Figs. 2(a)–(c). In Fig. 2(a), the Co thickness dependence of  $H_c$  change before and after sunlight illumination was systematically measured, and the maximum  $H_c$  change from 470 Oe (dark) to 410 Oe (2 suns illumination) appears at 0.7 nm Co thickness. When Co thickness goes lower to 0.5 nm, the PMA gradually disappears due to inevitable substrate roughness, decreasing  $H_c$  tunability. The substrate roughness is illustrated in Fig. S3. It demonstrates that higher surface roughness prevents the formation of thin-film heterostructure of PMA effect [Pt (0.8 nm)/Co (0.7 nm)/Pt (2.75 nm)]. As the Co thickness increases to 1 nm, the PMA strength enhances accordingly, resulting in a relatively small sunlight tunability. It attributes to the photo-induced electrons doping so that the Fermi level can be shifted to enhance the in-plane Rashba field within Co/Pt interfaces, resulting in weakened PMA according to our previous work [40].

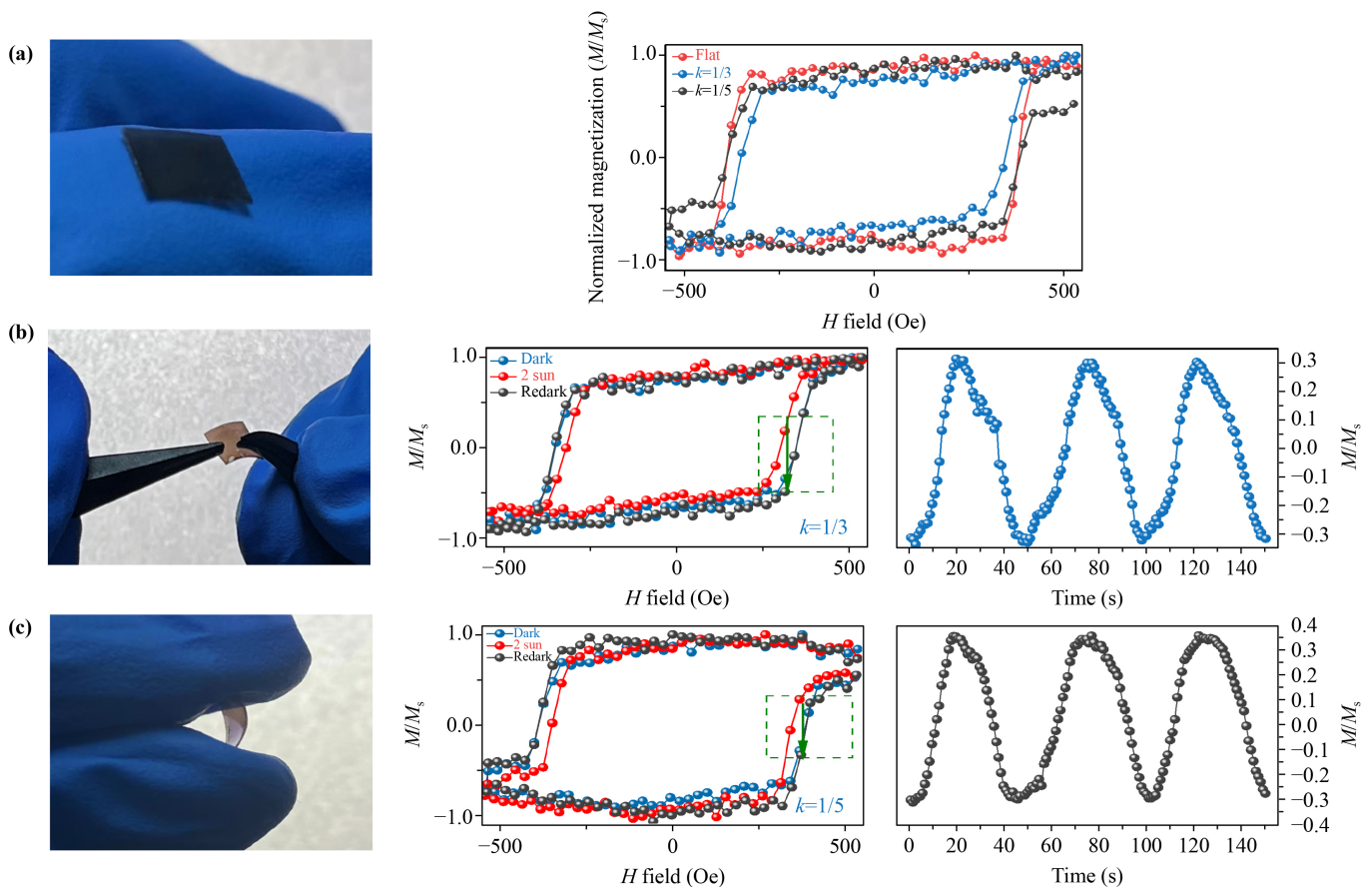


**Fig. 3** The sunlight control of PMA on flexible substrates under different bending conditions. **(a)** The magnetic hysteresis loop test of PV/PMA heterostructure under flat (red), bending (curvature = 1/3, blue; 1/5, black) conditions. **(b)** The magnetic hysteresis loop of PV/PMA heterostructure with and without sunlight illumination (dark, blue; redark, black) at substrate bending curvature 1/3. The magnetization switches by turning the sunlight on and off with magnetic bias. **(c)** The magnetic hysteresis loop of PV/PMA heterostructure with and without sunlight illumination (dark, blue; redark, black) at substrate bending curvature of 1/5. The corresponding sunlight-induced magnetization switches at magnetic bias.

Meanwhile, the angular dependence (the angle  $\theta$  between the applied magnetic field and device-film-plane) of  $H_c$  tunability is also investigated in Figs. 2(b) and S1 (Supporting Information). The maximum sunlight control of  $H_c$  tunability (from  $\sim 800$  Oe to  $\sim 500$  Oe, referring to 60% tunability) was obtained at  $\theta = 30^\circ$ . In contrast, at  $\theta = 0^\circ$  and  $90^\circ$ , the tunability decreases to zero. The large  $H_c$  tunability enables a sunlight control of deterministic magnetization switching with a slight magnetic bias, as in our previous work in PMA/P-N Si heterojunctions, where a near 180-degree sunlight tunable magnetization switching was achieved. However, the optimized magnetic field angle for magnetization switching in this experiment is not  $30^\circ$  because the  $M-H$  loop is highly tilted [40]. Here, we fixed the  $\theta = 70^\circ$ , where the tunability and the squareness of the  $M-H$  loop are balanced. As shown in Fig. 2(c), the  $M-H$  loop becomes compact, with  $H_c$  decreasing from 470 Oe (blue) to 410 Oe (red) under 2 suns illumination. While applying a magnetic bias of  $\sim 440$  Oe, the magnetization can be switched from negative (dark) to positive (light) with

good reversibility under sunlight, as presented in Fig. 2(d). Indeed, the PMA and magnetization switching angle tunability in the flexible substrate is not comparable to those on P-N Si. The reasons are attributed to the relatively large roughness and non-compensable residual stress of flexible PET substrates and the lower photoelectron generation rate of OPV than that of P-N Si.

In order to examine the stability of flexible PV/PMA devices under various strain/stress conditions, the  $M-H$  loops under flat and bending (with curvatures of 1/3 and 1/5, respectively) conditions are tested, as shown in Fig. 3(a). By bending the film, the loops of PMA effect can be altered due to the inverse magnetostriction effect. It attributes to the negative magnetostriction coefficient of cobalt [30]. The  $M-H$  loops vary as the bending curvature changes from flat to 1/3 and 1/5, respectively, proving a strain-induced magnetic anisotropy change. While the bending curvature maintains 1/3, as represented in Fig. 3(b), the  $H_c$  of the  $M-H$  loop still reversibly decreases under 2 suns illumination, which means that the  $M-H$  loop returns to its original after withdrawing

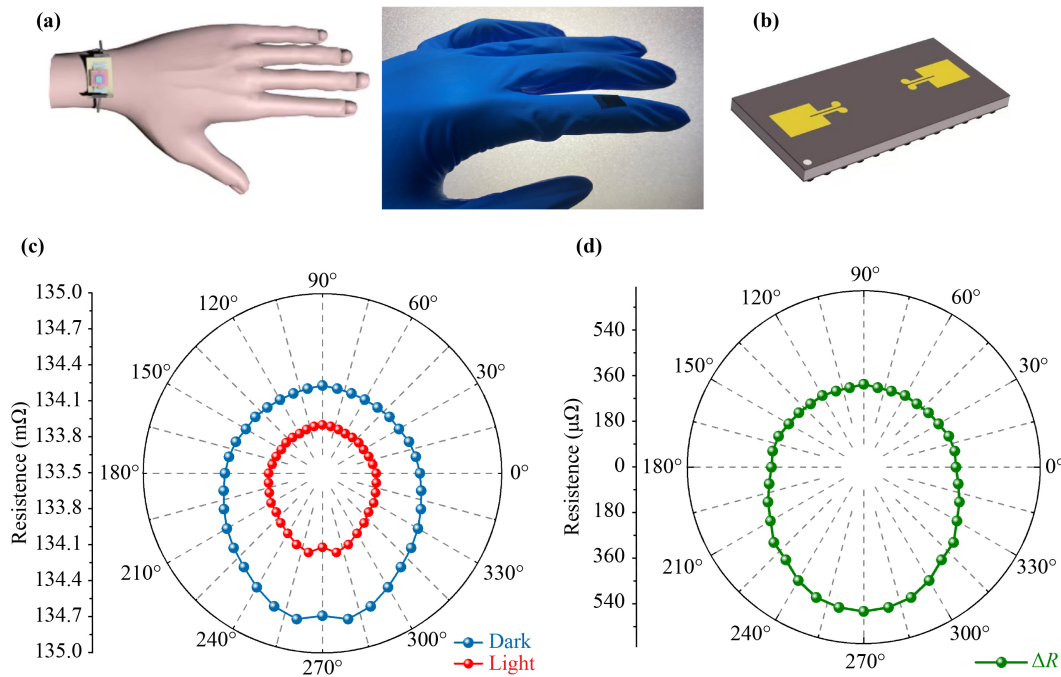


**Fig. 4** The prototype device of the solar-driven spintronic sensor. (a) The schematic and actual photo of the solar-driven rotating sensor on a human hand. (b) The schematic of electrodes on the PV/PMA heterostructures. (c) The angular dependence of voltage output with (blue) and without (red) sunlight illuminations. (d) The angular dependence of voltage output difference between light and dark conditions.

the sunlight. By applying  $\sim 420$  Oe magnetic bias, the magnetization also switches from negative (dark) to positive (light) back and forth as it is under flat conditions [Fig. 2(d)]. Similarly, at the bending curvature of  $1/5$  [Fig. 3(c)], both  $M-H$  loops,  $H_c$ , and magnetization switching at a fixed magnetic bias ( $\sim 380$  Oe) are tunable by sunlight with good reversibility, showing that the solar-driven PMA change, as well as magnetization switching, can be applied to flexible substrates with complex bending conditions for real flexible spintronic applications.

The angular dependence of sunlight-tunable magnetoresistance ( $M_R$ ) is also measured for real applications that the input and output signals are voltage or current. Figure 4(a) shows the schematic and actual photo of the prototype solar-driven spintronic sensor on a human hand for potential wearable electronics/spintronics. Figure 4(b) represents the two-point electrodes on the device for magnetoresistance testing. By rotating the applied external magnetic field  $360^\circ$  and fixing the magnetic field to 500 Oe, the angular  $M_R$  with (red) and without (blue) sunlight are summarized, showing a  $\sim 0.55$  mΩ  $M_R$  change at its maximum angle of  $270^\circ$  [Fig. 4(c)]. Figure 4(d) demonstrates the angular dependence of  $M_R$  under sunlight in a  $\sim 0.3$ – $0.55$  mΩ range. Although the  $M_R$  change is relatively small, solar-driven flexible spintronics is indeed feasible, and it will keep improving rapidly by optimizing the OPV efficiency, ferromagnetic heterostructure, and substrate selections.

## 4 Conclusion

In conclusion, we realized a solar-tunable PMA heterostructure flexible substrates, where the  $H_c$  can be effectively tuned by sunlight illumination from 470 Oe to 410 Oe with 14.6% tunability. With a slight magnetic bias of 320 Oe, magnetization orientation can be manipulated back and forth by turning the sunlight on and off, creating a “0” and “1” information unit. Under pending conditions ( $k = 1/3, 1/5$ ), the PV/PMA devices maintain effective sunlight tunability with strain/stress stability. Lastly, we tested a sunlight-tunable flexible sensor based on our structure, which demonstrated a good angular-dependent sunlight response and paved the way toward solar-driven flexible spintronics in the upcoming years.

**Declarations** The authors declare that they have no competing interests and there are no conflicts.

**Electronic supplementary materials** The online version contains supplementary material available at <https://doi.org/10.1007/s11467-023-1377-0> and <https://journal.hep.com.cn/fop/EN/10.1007/s11467-023-1377-0>.

**Acknowledgements** The work was supported by the National Key R&D Program of China (Grant No. 2022YFB3203903), the National Natural Science Foundation of China (Grant Nos. 52172126 and 62001366), and the China Postdoctoral Science Foundation (Grant No. 2022M722509).

## References

- X. T. Zheng, Z. Yang, L. Sutarlie, M. Thangaveloo, Y. Yu, N. Salleh, J. S. Chin, Z. Xiong, D. L. Becker, X. J. Loh, B. C. K. Tee, and X. Su, Battery-free and AI-enabled multiplexed sensor patches for wound monitoring, *Sci. Adv.* 9(24), eadg6670 (2023)
- Y. Zhao, R. Peng, Y. Guo, Z. Liu, Y. Dong, S. Zhao, Y. Li, G. Dong, Y. Hu, J. Zhang, Y. Peng, T. Yang, B. Tian, Y. Zhao, Z. Zhou, Z. Jiang, Z. Luo, and M. Liu, Ultraflexible and malleable Fe/BaTiO<sub>3</sub> multiferroic heterostructures for functional devices, *Adv. Funct. Mater.* 31(16), 2009376 (2021)
- Y. Cao, N. Wang, H. Tian, J. Guo, Y. Wei, H. Chen, Y. Miao, W. Zou, K. Pan, Y. He, H. Cao, Y. Ke, M. Xu, Y. Wang, M. Yang, K. Du, Z. Fu, D. Kong, D. Dai, Y. Jin, G. Li, H. Li, Q. Peng, J. Wang, and W. Huang, Perovskite light-emitting diodes based on spontaneously formed submicrometre-scale structures, *Nature* 562(7726), 249 (2018)
- S. Ota, A. Ando, and D. Chiba, A flexible giant magnetoresistive device for sensing strain direction, *Nat. Electron.* 1(2), 124 (2018)
- S. Park, S. W. Heo, W. Lee, D. Inoue, Z. Jiang, K. Yu, H. Jinno, D. Hashizume, M. Sekino, T. Yokota, K. Fukuda, K. Tajima, and T. Someya, Self-powered ultraflexible electronics via nano-grating-patterned organic photovoltaics, *Nature* 561(7724), 516 (2018)
- S. Bauer, Flexible electronics: Sophisticated skin, *Nat. Mater.* 12(10), 871 (2013)
- Y. Lei, Y. Chen, R. Zhang, Y. Li, Q. Yan, S. Lee, Y. Yu, H. Tsai, W. Choi, K. Wang, Y. Luo, Y. Gu, X. Zheng, C. Wang, C. Wang, H. Hu, Y. Li, B. Qi, M. Lin, Z. Zhang, S. A. Dayeh, M. Pharr, D. P. Fenning, Y. H. Lo, J. Luo, K. Yang, J. Yoo, W. Nie, and S. Xu, A fabrication process for flexible single-crystal perovskite devices, *Nature* 583(7818), 790 (2020)
- J. Viventi, D. H. Kim, L. Vigeland, E. S. Frechette, J. A. Blanco, Y. S. Kim, A. E. Avrin, V. R. Tiruvadi, S. W. Hwang, A. C. Vanleer, D. F. Wulsin, K. Davis, C. E. Gelber, L. Palmer, J. Van der Spiegel, J. Wu, J. Xiao, Y. Huang, D. Contreras, J. A. Rogers, and B. Litt, Flexible, foldable, actively multiplexed, high-density electrode array for mapping brain activity in vivo, *Nat. Neurosci.* 14(12), 1599 (2011)
- X. Cai, Y. Liu, J. Zha, F. Tan, B. Zhang, W. Yan, J. Zhao, B. Lu, J. Zhou, and C. Tan, A flexible and safe planar zinc-ion micro-battery with ultrahigh energy density enabled by interfacial engineering for wearable sensing systems, *Adv. Funct. Mater.* 33(29), 2303009 (2023)
- Y. Zhang, Y. Wang, C. Wang, Y. Zhao, W. Jing, S. Wang, Y. Zhang, X. Xu, F. Zhang, K. Yu, Q. Mao, Q. Lin, F. Han, B. Tian, Z. Zhou, L. Zhao, W. Ren, M. Liu, and Z. Jiang, Superior performances via designed multiple embossments within interfaces for flexible pressure sensors, *Chem. Eng. J.* 454, 139990 (2023)
- G. Dong, Z. Zhou, X. Xue, Y. Zhang, B. Peng, M. Guan, S. Zhao, Z. Hu, W. Ren, Z. G. Ye, and M. Liu, Ferroelectric phase transition induced a large FMR tuning in self-assembled BaTiO<sub>3</sub>:Y<sub>3</sub>Fe<sub>5</sub>O<sub>12</sub> multiferroic composites, *ACS Appl. Mater. Interfaces* 9(36), 30733 (2017)
- C. Wu, X. Pan, F. Lin, Z. Cui, Y. He, G. Chen, Y. Zeng, X. Liu, Q. Chen, D. Sun, and Z. Hai, TiB<sub>2</sub>/SiCN thin-film strain gauges fabricated by direct writing for high-temperature application, *IEEE Sens. J.* 22(12), 11517 (2022)
- L. Zhu, Switching of perpendicular magnetization by spin-orbit torque, *Adv. Mater.* 35(48), 2300853 (2023)
- H. Yang, M. Ormaza, Z. Chi, E. Dolan, J. Ingla-Aynes, C. K. Safeer, F. Herling, N. Ontoso, M. Gobbi, B. Martin-Garcia, F. Schiller, L. E. Hueso, and F. Casanova, Gate-tunable spin hall effect in an all-light-element heterostructure: Graphene with copper oxide, *Nano Lett.* 23(10), 4406 (2023)
- J. Han, P. Zhang, J. T. Hou, S. A. Siddiqui, and L. Liu, Mutual control of coherent spin waves and magnetic domain walls in a magnonic device, *Science* 366(6469), 1121 (2019)
- H. Fulara, M. Zahedinejad, R. Khymyn, A. A. Awad, S. Muralidhar, M. Dvornik, and J. Akerman, Spin-orbit torque-driven propagating spin waves, *Sci. Adv.* 5(9), eaax8467 (2019)
- X. Shao, C. Zhu, P. Kumar, Y. Wang, J. Lu, M. Cha, L. Yao, Y. Cao, X. Mao, H. Heinz, and N. A. Kotov, Voltage modulated untwist deformations and multispectral optical effects from ion intercalation into chiral ceramic nanoparticles, *Adv. Mater.* 35(16), 2370116 (2023)
- W. J. Peng, L. Wang, Y. J. Li, Y. J. Du, Z. X. He, C. Y. Wang, Y. F. Zhao, Z. D. Jiang, Z. Y. Zhou, and M. Liu, Voltage manipulation of synthetic antiferromagnetism in CoFeB/Ta/CoFeB heterostructure for spintronic application, *Adv. Mater. Interfaces* 9(14), 2200007 (2022)
- B. Peng, Q. Lu, H. Tang, Y. Zhang, Y. Cheng, R. Qiu, Y. Guo, Z. Zhou, and M. Liu, Large in-plane piezo-strain enhanced voltage control of magnetic anisotropy in Si-compatible multiferroic thin films, *Mater. Horiz.* 9(12), 3013 (2022)
- B. Prasad, Y. L. Huang, R. V. Chopdekar, Z. Chen, J. Steffes, S. Das, Q. Li, M. Yang, C. C. Lin, T. Gosavi, D. E. Nikonov, Z. Q. Qiu, L. W. Martin, B. D. Huey, I. Young, J. Iniguez, S. Manipatruni, and R. Ramesh, Ultralow voltage manipulation of ferromagnetism, *Adv. Mater.* 32(28), 2001943 (2020)
- C. Song, B. Cui, F. Li, X. J. Zhou, and F. Pan, Recent progress in voltage control of magnetism: Materials, mechanisms, and performance, *Prog. Mater. Sci.* 87, 33 (2017)
- J. M. Hu, Z. Li, L. Q. Chen, and C. W. Nan, High-density magnetoresistive random access memory operating at ultralow voltage at room temperature, *Nat. Commun.* 2(1), 553 (2011)
- S. Yang, J. W. Son, T. S. Ju, D. M. Tran, H. S. Han, S. Park, B. H. Park, K. W. Moon, and C. Hwang, Magnetic skyrmion transistor gated with voltage-controlled magnetic anisotropy, *Adv. Mater.* 35(9), 2208881 (2023)
- H. J. Kim, K. W. Moon, B. X. Tran, S. Yoon, C. Kim, S. Yang, J. H. Ha, K. An, T. S. Ju, J. I. Hong, and C.

- Hwang, Field-free switching of magnetization by tilting the perpendicular magnetic anisotropy of Gd/Co multilayers, *Adv. Funct. Mater.* 32(26), 2112561 (2022)
25. Z. Tan, J. de Rojas, S. Martins, A. Lopeandia, A. Quintana, M. Cialone, J. Herrero-Martin, J. Meersschant, A. Vantomme, J. L. Costa-Kramer, J. Sort, and E. Menendez, Frequency-dependent stimulated and post-stimulated voltage control of magnetism in transition metal nitrides: Towards brain-inspired magneto-ionics, *Mater. Horiz.* 10, 88 (2023)
26. M. Ameziane, R. Mansell, V. Havu, P. Rinke, and S. van Dijken, Lithium-ion battery technology for voltage control of perpendicular magnetization, *Adv. Funct. Mater.* 32(29), 2113118 (2022)
27. M. Huang, M. U. Hasan, K. Klyukin, D. Zhang, D. Lyu, P. Gargiani, M. Valvidares, S. Sheffels, A. Churikova, F. Buttner, J. Zehner, L. Caretta, K. Y. Lee, J. Chang, J. P. Wang, K. Leistner, B. Yildiz, and G. S. D. Beach, Voltage control of ferrimagnetic order and voltage-assisted writing of ferrimagnetic spin textures, *Nat. Nanotechnol.* 16(9), 981 (2021)
28. S. Zhao, Z. Zhou, C. Li, B. Peng, Z. Hu, and M. Liu, Low-voltage control of  $(\text{Co/Pt})_x$  perpendicular magnetic anisotropy heterostructure for flexible spintronics, *ACS Nano* 12(7), 7167 (2018)
29. S. Zhao, L. Wang, Z. Zhou, C. Li, G. Dong, L. Zhang, B. Peng, T. Min, Z. Hu, J. Ma, W. Ren, Z. G. Ye, W. Chen, P. Yu, C. W. Nan, and M. Liu, Ionic liquid gating control of spin reorientation transition and switching of perpendicular magnetic anisotropy, *Adv. Mater.* 30(30), 1801639 (2018)
30. B. Peng, Z. Zhou, T. Nan, G. Dong, M. Feng, Q. Yang, X. Wang, S. Zhao, D. Xian, Z. D. Jiang, W. Ren, Z. G. Ye, N. X. Sun, and M. Liu, Deterministic switching of perpendicular magnetic anisotropy by voltage control of spin reorientation transition in  $(\text{Co/Pt})_3/\text{Pb}(\text{Mg}_{1/3}\text{Nb}_{2/3})\text{O}_3\text{-PbTiO}_3$  multiferroic heterostructures, *ACS Nano* 11(4), 4337 (2017)
31. B. Peng, M. Feng, Q. Yang, S. Zhao, Y. Zhang, Z. Zhou, and M. Liu, Ferroelastic strain-mediated nonvolatile tuning of perpendicular magnetic anisotropy in  $(\text{Co/Pt})_3/(1\ 1\ 1)\ \text{Pb}(\text{Mg}_{1/3}\text{Nb}_{2/3})\text{O}_3\text{-PbTiO}_3$  multiferroic heterostructures, *IEEE Magn. Lett.* 8, 1 (2017)
32. Q. Yang, Z. Zhou, L. Wang, H. Zhang, Y. Cheng, Z. Hu, B. Peng, and M. Liu, Ionic gel modulation of RKKY interactions in synthetic anti-ferromagnetic nanostructures for low power wearable spintronic devices, *Adv. Mater.* 30(22), 1800449 (2018)
33. Q. Yang, L. Wang, Z. Zhou, L. Wang, Y. Zhang, S. Zhao, G. Dong, Y. Cheng, T. Min, Z. Hu, W. Chen, K. Xia, and M. Liu, Ionic liquid gating control of RKKY interaction in  $\text{FeCoB/Ru/FeCoB}$  and  $(\text{Pt/Co})_2/\text{Ru}/(\text{Co/Pt})_2$  multilayers, *Nat. Commun.* 9(1), 991 (2018)
34. X. Wang, Q. Yang, L. Wang, Z. Zhou, T. Min, M. Liu, and N. X. Sun, E-field control of the RKKY interaction in  $\text{FeCoB/Ru/FeCoB/PMN-PT}$  (011) multiferroic heterostructures, *Adv. Mater.* 30(39), 1803612 (2018)
35. Y. F. Zhao, Y. J. Du, L. Wang, K. Chen, Z. L. Luo, W. S. Yan, Q. Li, Z. D. Jiang, M. Liu, and Z. Y. Zhou, Sunlight-induced tri-state spin memory in photovoltaic/ferromagnetic heterostructure, *Nano Today* 46, 101605 (2022)
36. C. L. Li, Y. J. Li, Y. F. Zhao, Y. J. Du, M. Zhao, W. J. Peng, Y. Y. Wu, M. Liu, and Z. Y. Zhou, Sunlight control of ferromagnetic damping in photovoltaic/ferromagnetic heterostructures, *Adv. Funct. Mater.* 32(16), 2111652 (2022)
37. Y. J. Du, S. P. Wang, L. Wang, S. Y. Jin, Y. F. Zhao, T. Min, Z. D. Jiang, Z. Y. Zhou, and M. Liu, Improving solar control of magnetism in ternary organic photovoltaic system with enhanced photo-induced electrons doping, *Nano Res.* 15(3), 2626 (2022)
38. Y. Zhao, S. Zhao, L. Wang, S. Wang, Y. Du, Y. Zhao, S. Jin, T. Min, B. Tian, Z. Jiang, Z. Zhou, and M. Liu, Photovoltaic modulation of ferromagnetism within a FM metal/P-N junction Si heterostructure, *Nanoscale* 13(1), 272 (2021)
39. Y. Zhao, S. Zhao, L. Wang, Z. Zhou, J. Liu, T. Min, B. Peng, Z. Hu, S. Jin, and M. Liu, Sunlight control of interfacial magnetism for solar driven spintronic applications, *Adv. Sci. (Weinh.)* 6(24), 1901994 (2019)
40. M. Zhao, L. Wang, Y. Zhao, Y. Du, Z. He, K. Chen, Z. Luo, W. Yan, Q. Li, C. Wang, Z. Jiang, M. Liu, and Z. Zhou, Deterministic magnetic switching in perpendicular magnetic trilayers through sunlight-induced photoelectron injection, *Small* 19(28), 2301955 (2023)